

# High-temperature phase transitions, dielectric relaxation, and ionic mobility of proustite, $\text{Ag}_3\text{AsS}_3$ , and pyrargyrite, $\text{Ag}_3\text{SbS}_3$

Kristin A. Schönau

*Department of Earth Sciences, University of Cambridge, Downing Street, Cambridge CB2 3EQ, United Kingdom*

Simon A. T. Redfern<sup>a)</sup>

*Department of Earth Sciences, University of Cambridge, Downing Street, Cambridge CB2 3EQ, United Kingdom and Research School of Earth Sciences, Australian National University, Mills Road, Canberra, ACT 0200, Australia*

(Received 25 March 2002; accepted 20 September 2002)

The nature of phase transitions in natural and synthetic proustite,  $\text{Ag}_3\text{AsS}_3$ , has been studied in darkness above 300 K and compared with its natural counterpart pyrargyrite,  $\text{Ag}_3\text{SbS}_3$ . The behavior of proustite is characterized by silver ion mobility within the structure. Proustite and (to a lesser extent) pyrargyrite were investigated as a function of temperature by x-ray and neutron powder diffraction, dielectric spectroscopy, and dynamic mechanical analysis. At 305 K (280 K for pyrargyrite) proustite undergoes a second-order phase transition, exhibiting a positive nonsymmetry breaking spontaneous strain of the unit cell, with thermal expansion along [001] changing from negative to positive. This strain results from the onset of thermally induced hopping of silver ions, as revealed by impedance spectroscopy. It may be described as an almost undamped Debye oscillator, which is not present below  $T_c$  (305 K) with an activation energy of 0.42 eV (0.40 eV for pyrargyrite). Around 420 K the high-frequency conductivity of proustite begins to increase, accompanied by elastic softening. At this temperature increasing random disorder of silver within possible unoccupied sites in the structure leads to increased electrical conductivity and destabilizes the material. When almost all silver ions are disordered into a so-called “molten sublattice,” a transition to fast ion conduction (at 540 K in proustite and 490 K in pyrargyrite) is reached. The additional component to the thermal expansion disappears and a linear negative spontaneous strain suggests a second-order phase transition. Above the transition silver seems to be maximally disordered, the structure itself is weakened and the sample starts to decompose. © 2002 American Institute of Physics. [DOI: 10.1063/1.1520720]

## I. INTRODUCTION

Over the last few decades proustite,  $\text{Ag}_3\text{AsS}_3$ , has attracted considerable interest due to its physical properties and possible technological applications. Proustite is well known as an electro-optic crystal with nonlinear optical character. It is acentric as well as uniaxial, and can be used for optical mixing and second harmonic generation.<sup>1</sup> Its properties as a photosensitive semiconductor are used in acoustoelectronics<sup>2</sup> and optics, as well as in the field of dielectrics.<sup>3,4</sup>

Proustite,  $\text{Ag}_3\text{AsS}_3$ , and pyrargyrite,  $\text{Ag}_3\text{SbS}_3$ , belong to the group of complex sulphosalts  $\text{A}_x\text{B}_y\text{S}_n$ , where  $\text{A} = \text{Ag, Cu, Pb, etc.}$ , and  $\text{B} = \text{As, Sb, Bi}$ . Pure red, rhombohedral silver orthosulphoarsenite crystals were first described by Proust in 1804, after whom they were named as proustite. In nature, proustite almost always appears together with pyrargyrite and other silver bearing minerals and sulphides like argentite or acanthite (both  $\text{Ag}_2\text{S}$ ) in epithermal veins, which form silver ore deposits. The formation temperatures of the veins are mostly in the region of 573 to 673 K. Proustite and

pyrargyrite form a complete solid solution.<sup>5</sup> They are isostructural ( $R3c$ ), and have similar physical properties and crystal habit. A second, quite rare natural modification of  $\text{Ag}_3\text{AsS}_3$  is called xanthoconite, which is yellow and monoclinic ( $C2/c$ ).<sup>6</sup> It seems to be a less stable phase than proustite and changes structure irreversibly into proustite at  $465 \pm 10$  K through a reconstructive phase transition.<sup>7</sup> These phases lie in the ternary system  $\text{Ag-As-S}$  on the binary join  $\text{Ag}_2\text{S-As}_2\text{S}_3$ , and at high temperature decompose into these two end members.<sup>8</sup>

Proustite exhibits a variety of physical phenomena, which often can be assigned to particular temperature regions and are mostly related to optical and electrical properties. The structural properties, and especially the distribution of silver ions within the structure, play a major role in changes of physical behavior of the sample with temperature. The room-temperature structure of proustite was first described by Harker,<sup>9</sup> who found it to be trigonal, space group  $R3c$ . The arsenic and sulphur atoms form covalently bonded  $\text{AsS}_3$  pyramids occupying the  $C_3$  sites in the structure.<sup>10</sup> Alternate pyramids aligned along the polar threefold  $c$  axis are related to each other through a  $c$ -glide plane. Ag atoms reside in half of the possible  $C_1$  sites between the pyramids and corner link the  $\text{AsS}_3$  complexes ionically via  $\text{S-Ag-S}$  links, which

<sup>a)</sup> Author to whom correspondence should be addressed; electronic mail: [satr@cam.ac.uk](mailto:satr@cam.ac.uk)

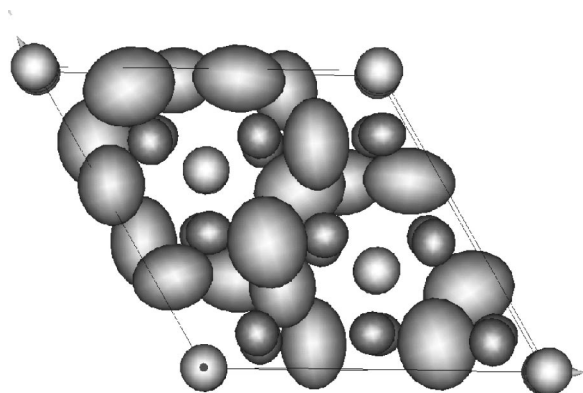


FIG. 1. Hexagonal unit cell of proustite according to Engel and Novacki (see Ref. 10) with thermal ellipsoids at 300 K, viewed along the threefold  $c$  axis. Silver ions are large and oval shaped, enclosing  $\text{AsS}_3$  pyramids with arsenic in their center and sulphur surrounding it on three sides.

themselves form two sets of three-sided  $(\text{AgS})_\infty$  helices of different handedness parallel to the  $c$  axis. The  $\text{AsS}_3$  pyramids linked by  $\text{Ag-S}$  bonds are related through translational symmetry only and not by the  $c$  glide. Thus, the structure can be thought of as two interwoven but unlinked substructures of pyramids and spirals related to each other via a  $c$  glide plane (Fig. 1). There are three types of nonintersecting  $\text{Ag}$  chains within the structure.

A semiconductor with an energy gap of around 2 eV at 290 K,<sup>4</sup> proustite undergoes changes in its conduction mechanisms, varying from electronic conductivity and pyroelectrical conduction at low temperatures<sup>11,12</sup> over different stages of mixed electronic and ionic conductivity with the ionic component dominating at temperatures in excess of  $\sim 230 \text{ K}^3$  to a fast ion conducting phase at high temperatures.<sup>4,13</sup> Some of these conduction mechanisms are strongly influenced by optical illumination. Below 28 K proustite is ferroelectric. The silver ions interact with other atoms ionically and are the mobile species in the structure. Many changes in characteristics, such as the ionic conduction in proustite and several suggested phase transitions, are related to the different stages of silver ion order-disorder. Silver has an oblate thermal vibration ellipsoid<sup>14</sup> and ionic conductivity is likely to take place through the chains of silver and the  $(\text{AgS})_\infty$  spirals in the structure, both being equally probable. Ewen and co-workers<sup>15</sup> linked this motion of silver closely to the existence of six alternative sites for silver ions, in which they can disorder. The  $\text{Ag}^+$  ions move in double-well potentials created by the remaining lattice in between the  $\text{S-Ag-S}$  spirals.

The low-temperature ferroelectric transition, further incommensurate behavior and structural transitions have been the subject of numerous studies.<sup>14-21</sup> An enigmatic second-order “phase transition” at 210 K, only occurring under illumination with white light, was claimed by Yang and Taylor.<sup>13</sup> At this transition many physical properties, such as the band gap energy, absorption coefficient and ionic conductivity, show anomalies, but no sign of a structural change was detected in x-ray, neutron, or nuclear magnetic resonance (NMR) experiments.<sup>13,14,16</sup> The proposed mechanism of this transition involves the redistribution of silver ions

within all 12 possible sites in the structure under the influence of illumination.<sup>22</sup> Up to 305 K proustite shows an anomalous dielectric relaxation process when illuminated, in which  $\epsilon'$  increases anomalously with decreasing temperature. Without illumination no relaxation process is detected.<sup>3</sup>

According to Yang and Taylor,<sup>4</sup> marked changes in dispersion occur at 305 K. Below this temperature the conductivity is strongly frequency dependent and the dc conductivity is determined by the  $\text{Ag}^+$  migration energies alone. The dominant defects are still nonstoichiometric interstitial  $\text{Ag}^+$  ions created by diffusion of silver ions excited by illumination through an interlayer of good ionic conductivity. It is stated that, above 305 K, the conductivity of nonilluminated samples becomes almost independent of frequency but dependent on temperature, and is determined by silver ion migration energy and interstitial silver ion formation energy, in which carrier concentration is thermally activated with low hopping rate and high carrier density.

It is reported that above 420 K the silver ions have sufficient thermal energy for superionic conduction, becoming randomly distributed within the lattice, with a change from point defect conduction to a “molten sublattice” of silver.<sup>4</sup> However, relatively little is known about any structural changes associated with the conductivity changes postulated by Yang and Taylor<sup>4,13</sup> at 305 K, nor the temperature of the transition to fast ion conduction. Beside a note that the structure does not change between 300 and 435 K in the article by Belyaev and co-workers,<sup>23</sup> there are no data available on the high-temperature structure, as all investigations (e.g., Ref. 14 and others) were carried out up to room temperature, and no comparisons between low-temperature and high-temperature behavior were made. No information about the temperature and frequency dependence of the dielectric behavior of proustite has been reported above room temperature. Even less information is to be found on pyrargyrite.

Here, we report the results of an investigation into the behavior of  $\text{Ag}_3\text{AsS}_3$  and  $\text{Ag}_3\text{SbS}_3$  through room temperature up to the limits of their stabilities using dielectric spectroscopy, x-ray and neutron powder diffraction, and dynamic mechanical analysis to define the structure, characteristics and phase transitions present in the high-temperature form of proustite, and make a comparison with its isostructural counterpart pyrargyrite.

## II. EXPERIMENTAL METHODS

### A. Sample synthesis

For the dry sulphide synthesis, stoichiometric proportions (with a slight sulphur excess) of elementary silver (Alfa Aesar, granule +60 mesh, 99.99%), sulphur (Alfa Aesar, flakes, 99.998%) and arsenic (Alfa Aesar, pieces 99.9998%) were mixed and fused together by heating in an evacuated silica glass tube. It was first kept just above the melting point of sulphur ( $T_m = 459 \text{ K}$ ) at around 473 K to pre-react the elements at a low vapor pressure, and then heated up to around 673 K; at this temperature the silver mobility is high enough for reaction and the arsenic is vaporized.

Sufficient reaction for applying the Bridgman-Stockbarger technique was achieved after leaving the sample



FIG. 2. Image of twinned natural proustite NPr1 under crossed polars.

at 673 K for two days. The pre-reacted sample was placed vertically in a Bridgman furnace to grow pure phase dense macrocrystalline to single crystal proustite according to previously described methods.<sup>24</sup> The samples were inspected visually by x-ray diffraction and electron microprobe analysis (EMPA). These showed them to be single phase, the EMPA confirming stoichiometric composition.

Two natural equivalents to the synthetic specimens were studied. The first one NPr1, used for almost all of the measurements of natural material, was taken from the collection of the Department of Earth Sciences, University of Cambridge, UK. It was a bright red single crystal approximately 10 mm×6 mm×0.5 mm in size. As the amount of this material was very limited, a second natural specimen Npr2 was used for low-temperature x-ray powder diffraction studies. It also came from the collection of the Department of Earth Sciences, University of Cambridge, UK, and was polycrystalline material enclosed in a piece of milky quartz. Natural samples of pyrargyrite from the same source were also studied for comparison (Npy1, Npy2).

The sample Npr1 was investigated using an optical microscope in orthoscopic mode with crossed polars and in conoscopic mode in order to examine the interference figures and determine the orientation of the sample's crystallographic axes. Images recorded with crossed polars revealed that the crystal, which seemed initially to be single crystal, was twinned in one direction, with the orientation of the domain walls at an angle of about 30°–45° to the surface of the thin section (Fig. 2). Conoscopic microscopy showed that the section was cut directly perpendicular to the optical axis of the sample, the threefold  $c$  axis of proustite. On rotating the stage, it was observed that the sample was not uniaxial throughout, but slightly biaxial. The acute bisectrix is still perpendicular to the surface of the thin section, but the size of this deviation from uniaxial was dependent on the twin domain analyzed. It is likely that the twinning could have been caused by an externally applied stress or growth variations which slightly changed the symmetry, as has recently been described for other mineral systems.<sup>25–29</sup>

## B. Impedance spectroscopy

In order to analyze the dielectric behavior of samples NPr1 and NPy1, dielectric frequency-dispersive spectro-

scopic measurements were carried out. A computer-based four-terminal impedance spectrometer was used (Hewlett-Packard HP4010 Impedance Analyzer Model 4192A LF), following the method of Palmer and Salje.<sup>30</sup> Measurements of capacitance  $C$  and conductance  $G$  were recorded over a temperature range of 286–600 K, ramped in steps of 4 K per measurement within a small purpose-built furnace and from 100 to 390 K within a CTI Cryogenics close cycle helium cryostat. An alternating field was applied with a frequency range of 10 Hz–13 MHz, using 123 frequencies in logarithmic steps. A polished disk of each sample (0.5 mm thick for proustite and 0.3 mm for pyrargyrite), each cut perpendicular to the  $c$  axis, was placed between two platinum plates serving as electrodes and connected using Ag paste. During the experiment the interior of the tube furnace was held under dry  $N_2$  purge. The samples showed no reaction with the silver paste after each experiment. Due to their sensitivity to light the specimens were always kept in total darkness, allowing a recovery period of 1–2 days after exposure to light, which was described as sufficient by Shcherbin *et al.*<sup>31</sup>

Natural specimens of proustite were measured in four cycles, each consisting of a heating and a cooling run in the furnace and in two heating cycles in the cryostat. The synthetic sample showed similar results for the natural sample. Experimental data were reproducible if the samples were not heated above 523 K. At this temperature, breakdown of the sample is caused by decomposition reactions and possibly a reaction with the silver paste. For comparison with proustite, the natural pyrargyrite specimen was measured in the furnace under equivalent conditions.

## C. X-ray diffraction

X-ray powder diffraction data was obtained using CPS120 Instrument Electronic (INEL) position sensitive detector (PSD) with  $Cu K\alpha_1$  radiation. Powdered samples were placed onto a platinum–rhodium heating element for high-temperature measurements, and compressed into a nickel sample holder for low-temperature measurements. A vacuum was applied within the furnaces, depressurising the sample chamber in the low-temperature machine down to  $10^{-3}$  bar, and in the high-temperature machine to  $5 \times 10^{-5}$  bar. Low-temperature measurements were carried out using a closed circulating He cryostat.

The temperature was measured by thermocouples located directly underneath the sample holders, and controlled by a Eurotherm controller. Spectra were collected by an INEL PSD, with a “step size” of  $2\Theta = 0.015^\circ$ . For the low-temperature measurements ordinary focus x-ray tubes were used with an applied current of 30 kV and 20 mA. Low-temperature spectra of proustite were acquired with a counting time of 10 000 s per temperature step with cooling steps of 10 K from 270 K down to 20 K for the natural sample NPr2 and with 7200 s in 5 K steps for the synthetic sample from 290 to 115 K. Natural pyrargyrite NPy2 was measured for 10 000 s in 10 K steps from 70 to 280 K. The high-temperature spectra of the natural proustite specimen NPr1 were measured in 10 K steps with counting times of 7200 s per step from 343 to 718 K, using a Bede microfocus x-ray

source with an applied current of 40 kV and 2 mA. Pyrargyrite NPy2 was measured with a counting time of 3600 s in 10 K steps from 343 to 623 K. Several room-temperature diffraction patterns were recorded using a Guinier diffractometer and on both the low-temperature and the high-temperature INEL machine. Data of synthetic proustite recorded with the same techniques showed equivalent results and will therefore not be considered further in this study. Silicon was used as an internal standard for all measurements. The x-ray data were evaluated and converted from channels into  $2\theta$  values using a polynomial fit and were then refined to obtain the cell parameters using the general structure analysis program (GSAS) for Rietveld refinement.<sup>32</sup>

#### D. Neutron diffraction

Total neutron scattering experiments were undertaken on the general materials diffractometer GEM at the pulsed neutron spallation source in ISIS, Rutherford Appleton Laboratory (RAL). ISIS neutron diffraction instrumentation and GEM in particular are described in detail elsewhere.<sup>33–35</sup> A RAL furnace was used for high-temperature experiments. Sample holders were pure vanadium cans with an internal diameter of 6 mm for the lower temperature runs (from 292 to 353 K) and 8 mm internal diameter cans with a 6-mm-internal-diam silica glass tube holding the powdered synthetic proustite at higher temperatures (up to 513 K). Thus we avoided danger of a reaction between mobile silver atoms and the vanadium at high temperatures. The sample was studied in short runs at 5 K steps from 293 to 513 K in order to determine unit cell parameters. No higher temperatures were measured to avoid decomposition.

#### E. Dynamic mechanical analysis (DMA)

Using a Perkin-Elmer dynamic mechanical analysis (DMA)–7, very small thermal expansions and low-frequency elastic compliances of crystals can be measured in three-point bending geometry. The static force is modulated by a dynamic force of chosen amplitude and frequency, ranging from 0.1 to 50 Hz. The amplitude  $u$  and the phase shift  $\delta$  of the resulting elastic response of a synthetic proustite sample (1.48 mm  $\times$  5 mm  $\times$  0.62 mm) were registered via inductive coupling with a resolution of  $\Delta u \approx 10$  nm and  $\Delta \delta \approx 0.1^\circ$ .<sup>36</sup> The applied static and dynamic force were 50 and 40 mN, respectively. The resulting complex strain in the sample is made up of an elastic and a viscous contribution, which allows us to break up the single modulus in a term related to the storage of energy and one related to the loss of energy. The elastic or storage modulus is ideally the Young's modulus. The tangent of the phase angle  $\tan \delta$ , also termed damping or  $Q^{-1}$ , is an indicator of how efficiently the material loses energy to molecular rearrangements and internal friction, and is independent of the sample geometry.<sup>37</sup> Data were measured from 293 to 513 K scanning from 10–50 Hz every 5 K in steps of 0.2 Hz.

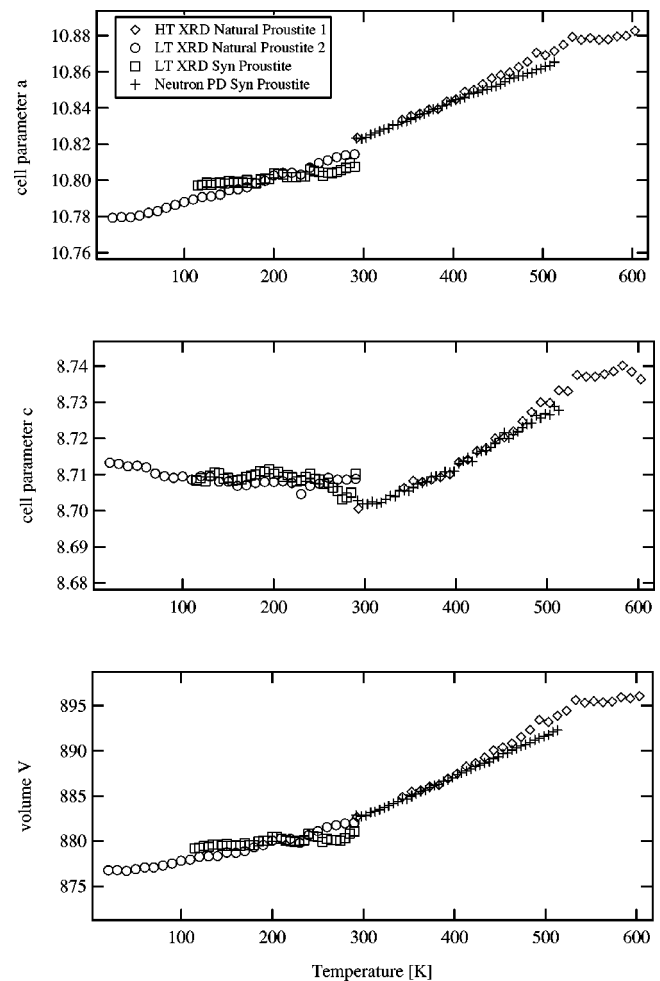


FIG. 3. The temperature-dependent lattice parameters and unit cell volume for natural proustite (NPr1 and NPr2) and synthetic proustite determined from x-ray and neutron powder diffraction data from 70 to 600 K using the Rietveld method. Cell parameters are given in Å and the unit cell volume in Å<sup>3</sup>. The errors in the data are smaller than the symbols used.

### III. EXPERIMENTAL RESULTS

#### A. Diffraction experiments

For Rietveld refinement x-ray patterns were all calibrated to the Si internal standard, and the cell parameters determined by neutron diffraction were then calibrated with reference to the room-temperature x-ray measurement. As a starting model in GSAS, the data of Engel and Nowacki<sup>10</sup> were used. Two anomalies can be seen in the cell parameter evolution in the region of interest between 250 and 600 K. For both the natural and the synthetic proustite samples, there are anomalies in the thermal expansion of the cell edges and the unit cell volume. These are seen as changes in the slope of the cell edge variation with temperature (Fig. 3); one at 305 K in both samples, and another at 540 K in the samples used for x-ray study (beyond the temperature range of the neutron study). Anomalies were found in the dielectric spectroscopy results at the same temperatures (see later). Proustite exhibits negative thermal expansion along  $c$  below room temperature, as reported previously,<sup>14</sup> which changes to a positive value above room temperature.

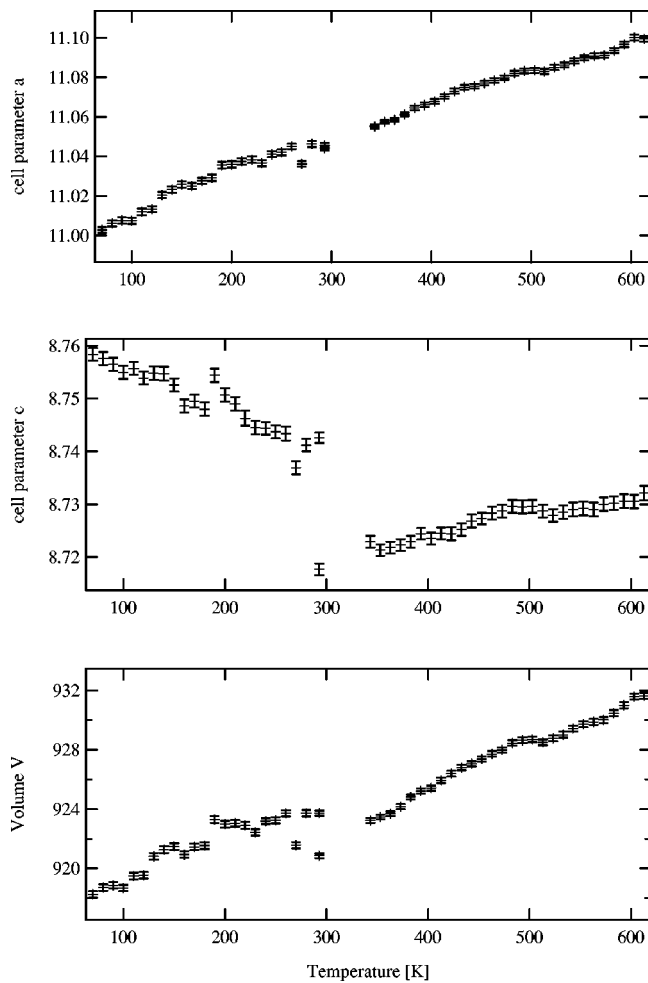


FIG. 4. The temperature-dependent lattice parameters and unit cell volume of natural pyrrargyrite, determined from x-ray powder diffraction. The offset between room-temperature measurement on the low-temperature and high-temperature data set is due to instrument differences. Cell parameters are given in Å and the unit cell volume in Å<sup>3</sup>.

Data for pyrrargyrite were collected on the high-temperature and low-temperature INEL machines in exactly the same way as those of natural proustite. The general features and behavior are similar, although the change to the high-temperature region is seen at lower temperature of around 490 K (Fig. 4) and the negative thermal expansion along *c* is greater in magnitude, while the changes in slope in *a* and *V* are smaller, all changing to a positive value at 280 K.

### B. Impedance spectroscopy

The measurements of proustite obtained from the impedance analyzer can be divided into two frequency regions displaying different behavior. A low-frequency region lies below approximately 5 kHz at room temperature, while a higher frequency region exists from 5 to 13 000 kHz, the highest frequency measurable by the apparatus. The capacitance, *C*, is much higher in the low-frequency region than in the high-frequency region (Fig. 5). In the low-frequency region, the conductance, *G*, is very low at all temperatures and hardly changes during the measurement. In contrast, the con-

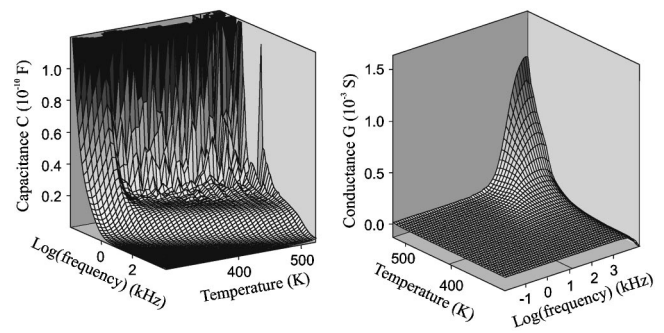


FIG. 5. Capacitance *C* (left) and conductance *G* (right) of natural proustite as a function of temperature and frequency of applied field.

ductance at higher frequencies increases dramatically to higher values at around 420 K and shows a jump at 490 K, reaching still higher values. Measurements made with the cryostat between 110 and 400 K show that the conductance below room temperature is very low and starts to increase slightly in the high-frequency region giving values equivalent to the values obtained in the furnace at the same temperature. The onset of the plateau in *C* above 300 K was confirmed. No other significant features of *G* and *C* could be detected below 300 K.

If an ac potential is applied across our sample, a phase shift  $\theta$  between the current and the voltage is induced due to the time dependence of the polarization processes. If the current *I* and the voltage *V* are considered to have a time variation of  $e^{i\omega t}$ , the quantity *V*/*I* is a complex number with no time dependence, and is called the *complex impedance Z*, the real part of which may be interpreted as a resistance, and the imaginary part may be interpreted as a capacitance

$$\frac{1}{Z} = G + i\omega C.$$

The term *impedance Z* is used to refer to the modulus of the *complex impedance Z*. The energy absorbed by the system in an oscillation processes can be measured by the *dielectric loss*,  $\tan \delta$ , with  $\delta = 90^\circ - \theta$ . It reaches its maximum at characteristic frequencies of the sample and is directly related to the real and the imaginary part of the dielectric permittivity,  $\epsilon'$  and  $\epsilon''$ . In an ac field with frequency  $\omega$

$$\tan \delta = \frac{\epsilon''}{\epsilon'} = \frac{G}{C\omega}.$$

We have used these relations to calculate the impedance, *Z*, and the dielectric loss,  $\tan \delta$ , of our samples as a function of temperature and frequency. The impedance, *Z*, shows several characteristic features. In the high-frequency region it stays constantly low without significant change over a range of temperatures. In the low-frequency region, at around room temperature, *Z* is over  $3.4 \times 10^7 \Omega^{-1}$ , and suddenly drops to a local minimum around 300–315 K. It then reaches another maximum of up to  $6 \times 10^6 \Omega^{-1}$  at around 360–380 K, finally dropping to a lower level above 420 K and reaching similar values as in the high-frequency region at 480–490 K (Fig. 6). It is worth noting that the separation of the high-frequency and the low-frequency region seems to be tem-

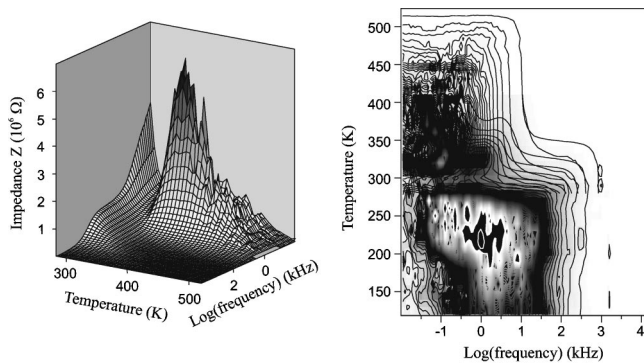


FIG. 6. (left) The modulus of the impedance,  $Z$ , in  $1/\Omega$  of natural proustite as a function of temperature and frequency. (right) Contour plot of  $Z$  of natural proustite combining both the high- and the low-temperature measurement.

perature independent. Below 300 K this boundary is at a higher frequency (around 100 kHz) than the boundary observed above 340 K (where it is seen around 5 kHz). It would seem likely that the frequency-independent minimum at around 305 K is due to a structural phase transition.

The behavior of  $\tan \delta$  is strongly temperature dependent in both the low-frequency and the high-frequency region, as shown in Fig. 7. Although the low-frequency region is noisy, the definitive feature is the sudden increase in  $\tan \delta$  at about 490 K. At higher frequencies, a constant sequence of maxima evolves out of a broad ridge that is seen around 305 K across a broadband of lower frequencies. At 305 K there is a resonance peak at about 1 kHz, which gently shifts as a set of maxima with increasing temperature to higher frequencies. The value of the maximum in this peak remains approximately constant between 330 and 490 K, then reduces to a lower value, and finally above 550 K  $\tan \delta$  increases to infinity. At this point it is likely that the sample breaks down into silver sulphide and arsenic compounds. These maxima in  $\tan \delta$  are not seen below room temperature, where the only peak observed was attributed to a resonance in the cryostat.

Dielectric measurements of the crystal of natural pyrrargyrite cut perpendicular to the  $c$  axis show similar features to those of proustite. The conductance increases in the high-frequency region at temperatures above 420 K while at the same time the impedance in the low-frequency region de-

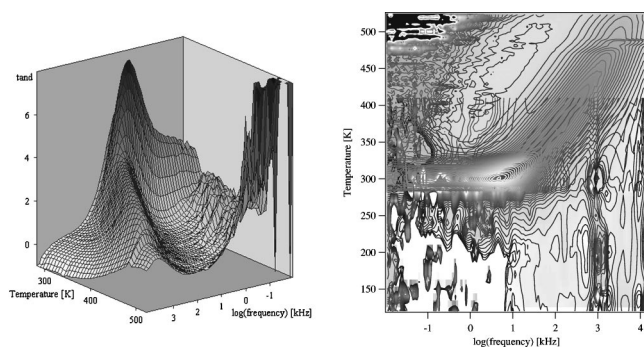


FIG. 7. Dielectric loss  $\tan \delta$  of natural proustite. The onset of a set of maxima from the ridge around 305 K is visible, and is absent below 305 K. The peak around 1000 kHz at low temperatures is an artifact, resulting from a resonance in the cryostat.

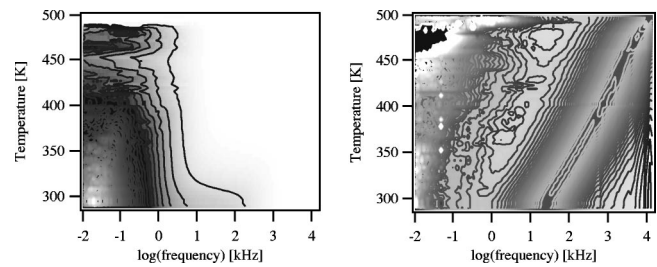


FIG. 8. Impedance (left) and dielectric loss (right) of pyrrargyrite as a function of temperature and frequency.

creases. The capacitance shows a similar plateau to that of proustite, and  $\tan \delta$  exhibits a series of maxima which shift to higher frequency values with increasing temperature at the same rate as in proustite (Fig. 8). Nevertheless, some differences could be detected: there is no local minimum in  $Z$  around 305 K, nor is there a frequency-independent ridge in  $\tan \delta$  here, nor is the onset of the plateau in the capacitance. These may be shifted to lower temperatures, as indicated by the onset of increased  $Z$  at higher frequencies around room temperature, but measurements were not undertaken using the cryostat.

### C. Dynamic mechanical analysis

To summarize the temperature dependence of the mechanical response of proustite, the frequency-dependent data between 10 and 50 Hz were combined (to reduce statistical noise). Just above 305 K the storage modulus, essentially the Young's modulus for proustite, displays a minimum as a function of temperature (Fig. 9). The dissipation function  $\tan \delta$  lies around zero at, and above, this temperature, until around 420 K, when a gradual increase takes place, associated with viscoelastic loss. This shows the same general trends as the increase in conductance measured by impedance spectroscopy (Fig. 5). When the final increase to a maximum in the viscous loss takes place, the material softens and finally it breaks down just above 500 K.

## IV. DISCUSSION

Before discussing the results one has to bear in mind the numerous previous investigations. In our search of the litera-

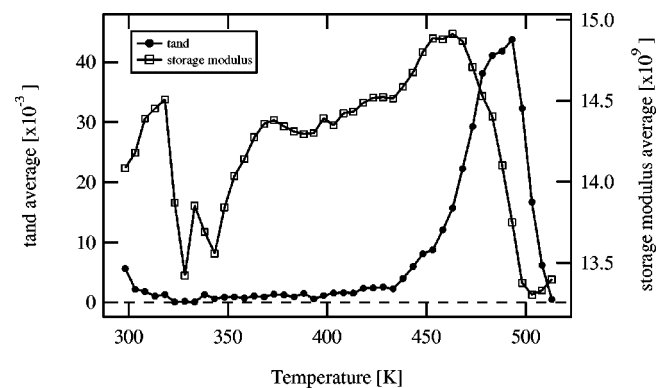


FIG. 9. Low-frequency (10–50 Hz) elastic loss and storage modulus of proustite as a function of temperature.

ture, no full structural data on proustite above 300 K by x-ray diffraction or neutron diffraction have been found. The space group of proustite at room temperature is reported as  $R3c$ . An interesting characteristic<sup>14</sup> confirmed here is the anomalous negative thermal expansion in the  $c$  axis up to room temperature. Proustite's dielectric behavior, and its dependence on illumination by light, was measured by Yang and Taylor.<sup>3,4</sup> They found that proustite exhibits anomalous dielectric relaxation under illumination with white light at  $T < 305$  K:  $\epsilon'$  increases anomalously with decreasing temperature. This behavior coincides with the assumption of Subramanian *et al.*<sup>21</sup> proposed in their NMR, where they have found the onset of  $\text{Ag}^+$  diffusion motions at about 240 K just above the broad transition of Yang and Taylor.<sup>4</sup> Unfortunately, Subramanian *et al.*<sup>21</sup> did not state whether or not their experiments were undertaken in darkness or under illumination, as the system is highly influenced in its characteristics by illumination. In darkness, no Debye relaxation is seen by us at  $T < 305$  K and there was no maximum observed in the dielectric loss function and  $\epsilon''$ ,<sup>3</sup> as is confirmed in this study. Yang and Taylor<sup>3,4</sup> did not undertake measurements above room temperature. They suggested that the electrical conductivity below 305 K was strongly frequency dependent, while above 305 K it becomes dependent only on temperature, controlled by silver ion migration energy and the interstitial silver ion formation energy. In this model the carrier concentration is thermally activated with low hopping rates and high carrier density. They detected another change in electrical conductivity at around 420 K which they interpreted (in terms of a first-order phase transition) as a change-over from  $\text{Ag}^+$  hopping between particular interstitial sites to fast ion conduction.

If changes in the structure of a material take place, such as redistribution of atoms between possible sites, to such an extent that it undergoes a structural phase transition, a spontaneous strain can develop in the low-temperature phase with respect to the high-temperature phase. This may be seen in the temperature evolution of the lattice parameters and volume, as deviations from the normal thermal expansion of the material. Even if there is no symmetry change, a volume strain can be present. These strains can be extracted from cell-parameter data to provide information about the course and character of the transition from the behavior of the order parameter,  $Q$ . Proustite and pyrargyrite both develop spontaneous strains at two distinct temperatures, one around room temperature and one at about 500 K. For pyrargyrite two transitions are apparent ( $T_c = 280$  and 490 K), at slightly lower transition temperatures than those in proustite (305 and 540 K). These are seen in changes in the temperature evolution of the cell parameters (Figs. 3 and 4). The corresponding spontaneous strains, determined as deviations from the behavior of the paraphase cell parameters, are shown in Fig. 10 for proustite and Fig. 11 for pyrargyrite. Changes in the lattice parameters are particularly clear in the  $T$  dependence of  $c$  in both minerals, with a change from negative thermal expansion below room temperature to positive expansion above  $T_c$  at 305 and 280 K, respectively.

As there are no stepwise discontinuities in any of the spontaneous strains, their changes being continuous, from

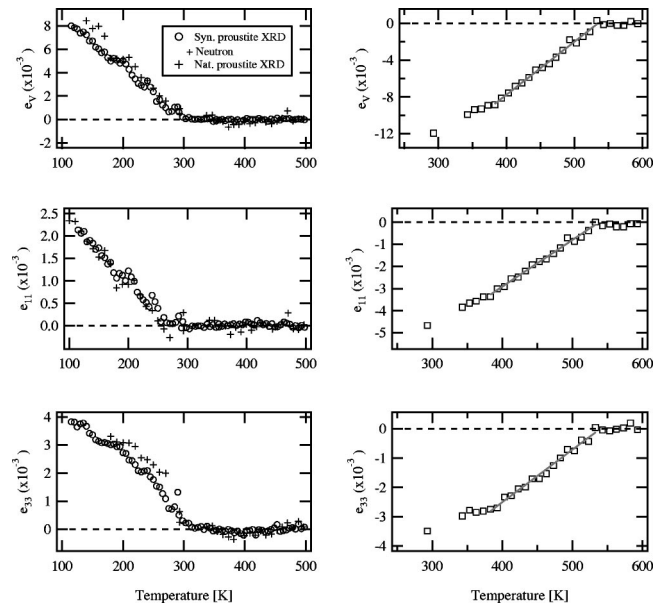


FIG. 10. (left) Positive strains developing in synthetic and natural proustite at the second-order phase transition at 305 K show a linear behavior below  $T_c$ , being continuous at  $T_c$ . (right) Linear negative strains in natural proustite at the transition at 540 K, which is also of second-order character.

zero in the high-temperature phases to a linear  $T$ -dependent behavior in the low-temperature phase, with  $e_i \propto (T_c - T)$ . The proportionality of the strain to the order parameter could be linear or quadratic, depending on the form of the symmetry change. We do not know the symmetry relations of the low and high phases, but since the strains along the cell edges behave in the same way as the volume strain (which, by symmetry, can only couple in the lowest order quadrati-

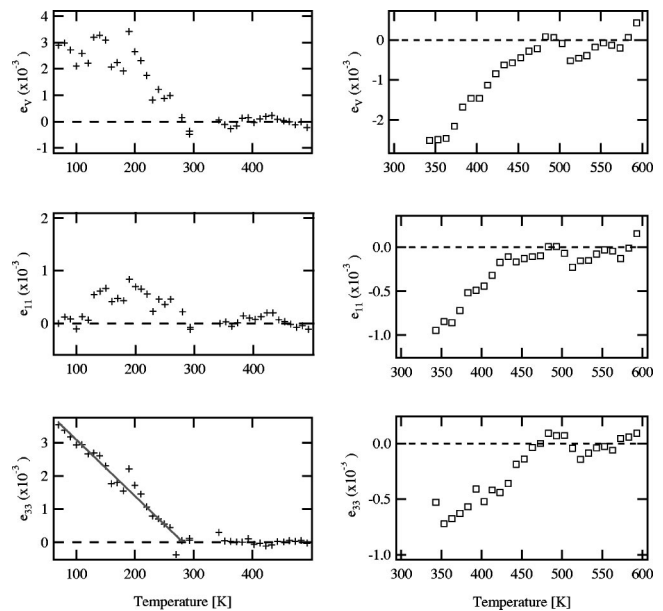


FIG. 11. (left) Positive strains developing in natural pyrargyrite at the second-order phase transition at 280 K show a linear behavior below  $T_c$  (seen best in  $e_{33}$ ), being continuous at  $T_c$ . The strain  $e_{11}$  is very weak and scatter in the data is very high, with errors increasing with distance from  $T_c$ . (right) Linear negative strain of pyrargyrite developing below the second-order phase transition at  $T_c = 490$  K.

cally with  $Q$ ), this suggests that they are proportional to the square of the order parameter  $Q$ , i.e.,  $e_i \propto Q^2$ . Thus the strains indicate that for all transitions observed  $Q^2 \propto (T_c - T)$ , suggesting a second-order character. The polarity of the spontaneous strains in different temperature regions is different, being positive at the lower transition which leads to an increased thermal expansion above  $T_c$ , and negative at the higher transition, where the thermal expansion behavior decreases in the high phase in relation to the low phase.

From the behavior of the impedance  $Z$  (Fig. 6) we can see that the regions of local and absolute minima are at exactly the same temperatures as the  $T_c$ s derived from x-ray and neutron powder diffraction. This suggests that the changes in cell parameters are linked to the conducting species within the structure as they undergo changes in behavior and ordering, increasing the conductivity during the transition to the high-temperature phase over that of the low-temperature phase. This is seen from the maximum values of the impedance  $Z$  in the low-frequency region, which decrease at each transition. Hence, the boundary of the region of low impedance at higher frequencies shifts to lower values. In the highest- $T$  phase, this leads to a dramatic increase in the conductance of proustite above 420 K (at high frequencies), as has been noted previously.<sup>4</sup> However, the conductance increases still further, up to 540 K, where the sample then breaks down into silver sulphide and arsenic sulphide, and does not remain static at the level of 420 K, where Yang and Taylor<sup>4</sup> suggested a first-order phase transition. No latent heat was found at around 420 K in differential scanning calorimetry measurements that we undertook on our samples. Furthermore, changes in the thermal expansion appear only at 540 K. This casts doubt on the previous<sup>4</sup> interpretation, and suggests that 420 K represents an onset temperature for increasing ionic conductivity, leading to a fast ion conducting phase. At 305 K no latent heat was detected either, which is consistent with the transition character being second order as suggested by the spontaneous strain behavior.

No dielectric relaxation process is observed below room temperature when the sample is kept in darkness, and the imaginary part of the dielectric constant  $\epsilon''$  and  $\tan \delta$  do not exhibit a maximum.<sup>3</sup> In our measurements, undertaken in the cryostat, the onset of a frequency-independent dielectric relaxation process associated with the silver ions is clear. This appears as a ridge in  $\tan \delta$  at 305 K (for frequencies below 5 kHz), while  $Z$  exhibits a minimum. The system also shows a resonance below 1 kHz, which shifts with increasing temperature to higher frequencies, which can be assigned to oscillation of the silver ions. Both  $\tan \delta$  and  $\epsilon''$  have a Lorentzian shaped maximum, while  $\epsilon'$  has a plateau equal to that of the capacitance  $C$  seen in Fig. 5. These features are characteristic for a Debye oscillator.

One possible explanation for these observations is that while the silver ions resided in distinct sites below 305 K (without illumination), above this temperature they have enough thermal energy to start to move (in darkness) between unoccupied  $C_1$  sites within the structure. They, therefore, hop between multi-well potentials with an activation energy of 0.42 eV (calculated from the dependence of the

characteristic relaxation time given by the peak in  $\tan \delta$  on  $1/T$  for our measured data). The onset of this process claimed by Subramanian *et al.*<sup>21</sup> at 240 K could not be confirmed in our investigation in darkness. An explanation for their measurement could be that their diffusion measured below room temperature is a similar characteristic to the onset of the fast ion conduction at 420 K where the number of disordered  $\text{Ag}^+$  slowly increases up to the transition temperature. However, our measurements show that there is no sloping in the impedance as a sign of a gradual onset but a distinct minimum at 305 K, as well as a dielectric loss equivalent to a relaxation process over a range of frequencies with the onset of a resonance corresponding to the silver hopping motion.

On heating, the oscillation process continues up to the decomposition  $T$  of the sample. The activation energy of the equivalent relaxation process observed in pyrrargyrite is 0.40 eV, almost the same as that of proustite, which confirms the hypothesis that the hopping motions are linked to the silver ions and not to the  $\text{AsS}_3$  or  $\text{SbS}_3$  groups.

In many dielectrics there is not just one single relaxation process (and hence relaxation time) involved. Instead there is a distribution of relaxation times and therefore of activation energies. For example, these may be due to different relaxation processes operating, or even to a distribution in the concentration of dipoles. In ionic hopping processes, such as those occurring in proustite, it can be assumed that immediately after an ion hops across a lattice potential energy surface to a new minimum it is still displaced from the true minimum in potential energy, which includes a contribution from other mobile defects. Over a long relaxation time this defect cloud relaxes until the true minimum coincides with the configuration. So a range of relaxation times may be present.<sup>38</sup>

To check how close the relaxation time of the process in proustite is to the single relaxation time assumed in the Debye model, the real and imaginary part of the dielectric constant can be plotted against each other in a Cole–Cole or Cole–Davidson plot, which gives the frequency dependence of the dielectric constant at a certain temperature. In the ideal Debye case this is a perfect semicircle bounded at  $\epsilon_s$  and  $\epsilon_\infty$  with a radius of  $(\epsilon_s - \epsilon_\infty)/2$ . The broader the distribution of relaxation times, the more the plot deviates from the semicircular Debye case. The deviation can be calculated with the empirical Havriliak–Negami expression for the frequency-dependent dielectric constant

$$\epsilon(\omega) = \epsilon_\infty + \frac{(\epsilon_s - \epsilon_\infty)}{(1 - (i\omega\tau)^{1-\alpha})^\beta}$$

Here, the parameters  $\alpha$  and  $\beta$  are a measure of the distortion of the semicircle, either depressing the center of the circle below the real axis, as examined in the Cole–Cole equation ( $\beta = 1, 0 < \alpha < 1$ ), or skewing it, seen in the Cole–Davidson expression ( $\alpha = 0, 0 < \beta < 1$ ). The values of  $\alpha$  and  $\beta$  lie between zero and one, and Debye-like behavior corresponds to  $\alpha = 0$  and  $\beta = 1$ . Fits were made for several temperatures and are reported in Table 1 and are illustrated in Fig. 12. Significant changes in  $\alpha$ ,  $\epsilon_s$  and  $\epsilon_\infty$  are seen with changing temperature. They increase in magnitude from an almost constant level upon the onset of increased  $\text{Ag}^+$  migration above

TABLE I. Parameters obtained from a Cole–Cole fit of dielectric constant data at various temperatures.

Temperature (K)	$\alpha$	$\beta$	$\epsilon_s$	$\epsilon_\infty$
373	0.016	0.907	3580	39.13
388	0.020	0.887	3590	38.10
417	0.018	0.868	3620	37.23
433	0.021	0.845	3680	46.45
453	0.029	0.861	3690	75.02
473	0.026	0.856	3750	139.0
489	0.046	0.866	3860	288.5
500	0.088	0.908	4020	469.3
510	0.222	0.707	4430	677.7

470 K. At temperatures above 500 K the parameters change as the system approaches a fast ion conductor. The changes in,  $\epsilon_\infty$ , which accompany the changeover, may be linked to increasing disorder of silver, which proceeds to a liquid-like state.

Within the errors of the fit it is clear that proustite shows an almost ideal Debye oscillation process with a small distribution of relaxation times, according to the Cole–Davidson model. The semicircle (Fig. 12) is not depressed and just very slightly skewed to the higher values of  $\epsilon'$ . This means that the hopping motion of the silver ions between Frenkel defects in the structure between 305 and 540 K is hardly disturbed and that the behavior is well described by a single relaxation process.

The results of the DMA experiment are consistent with the hypothesis advanced above: In the temperature region in which the Debye process (associated with hopping motions between possible sites) dominates—between 305 and 420 K—proustite behaves elastically and hardly any anelastic loss is seen. Since hopping produces a positive excess volume in the structure, it introduces a nonsymmetry breaking strain and the thermal expansion of proustite increases to higher values than seen at lower  $T$ , as seen in the positive spontaneous strain of the second-order phase transition at 305 K. However, above 420 K the number of  $\text{Ag}^+$  ions with enough thermal energy to move randomly within the structure (instead of exhibiting single hopping motions) slowly but constantly increases. The ionic  $\text{Ag}-\text{S}$  bonds between the  $\text{AsS}_3$  pyramids are broken and the silver ions start to randomly

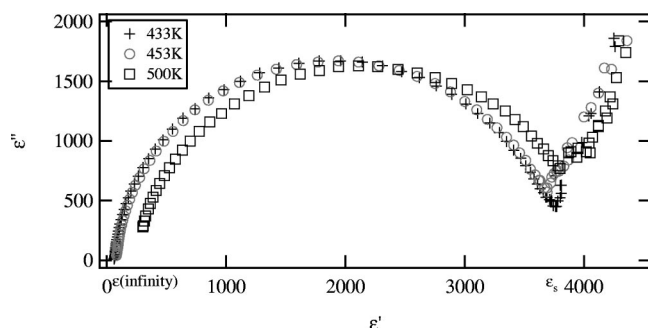


FIG. 12. Cole–Cole plot for our data from natural proustite at 433, 453, and 500 K. The huge increase in  $\epsilon''$  seen for high values of  $\epsilon'$  is associated with the noise in the low-frequency region of the dielectric spectra, and is not related to the Debye oscillation process.

disorder within the structure. The material softens and shows anelastic behavior, seen in the increase in mechanical  $\tan \delta$  (which mirrors  $\epsilon_\infty$ ) and the decrease in storage modulus. As more silver ions enter this “molten sublattice” of silver within the structure, it becomes less stable, and finally starts to break down at 540 K when most of the silver is disordered. At this point the transition to fast ion conduction is reached, with the remaining  $\text{Ag}^+$  ions insufficient to link the pyramids together. With maximum disorder of silver above 540 K within the structure, the additional contribution to the thermal expansion due to increasing disorder is diminished and the system returns to lower thermal expansion (similar to that seen before silver mobilization), giving the negative spontaneous strain at the second-order transition at 540 K. Above 540 K the sample starts to decompose, leaving residual  $\text{Ag}_2\text{S}$  while the other components vaporize. The more limited data we have on pyrargyrite all point to analogous behavior to proustite, with a slight depression of the temperatures of the phase transitions around room temperature and 500 K. It is worth reemphasising that the 305 K transition seen in proustite (280 K in pyrargyrite) was observed by us for samples held in darkness, and this may be related to the lower temperature anomalies seen previously<sup>4</sup> at 210 K for samples that were illuminated. It remains to be seen whether the behavior of pyrargyrite is light dependent.

## V. CONCLUSIONS

This study has shown that the high-temperature behavior of proustite is characterized by silver ion order–disorder within the structure. The same can be said for pyrargyrite, the behavior of which has been compared to that of proustite and found to be equivalent. It can be thought of as a minor deviation from that of proustite. Linked to the silver ion mobility, the properties of proustite change at various temperatures, resulting in different phases with various characteristics. These can be summarized within the model described in this work as:

(a) In darkness, at 305 K (around 280 K for pyrargyrite) proustite undergoes a second-order phase transition, evident from the positive nonsymmetry breaking spontaneous strain of the unit cell and the change in thermal expansion behavior. The negative thermal expansion along [001] becomes positive, as silver ions start hopping between unoccupied sites within the structure, leading to an additional component to the normal thermal expansion.

(b) The hopping motion is thermally activated as can be seen from impedance spectroscopy. It may be described by a single dielectric relaxation process, which appears in the form of an almost undamped Debye oscillator with an activation energy of 0.42 eV. This is not observed below the transition at 305 K. A Cole–Cole plot shows no distribution of relaxation times.

(c) At around 420 K the high-frequency electrical conductivity of proustite starts to increase, accompanied by a softening of the elastic modulus as revealed by DMA measurements. At this temperature, some of the silver ions, which previously just exhibited hopping motion, start to randomly disorder within the material and destabilize the struc-

ture. This leads to an increase in conductivity and to the onset of fast ionic conductivity.

(d) As silver positional disorder increases, the conductivity increases, and when almost all silver is disordered into a molten sublattice, a second phase transition (at 540 K in proustite and 490 K in pyrrargyrite) occurs. The additional component to the thermal expansion from silver disorder ceases and a linear negative spontaneous strain indicates that the transition is of second-order character. Above the transition silver seems to be maximally disordered within all possible sites, and the structure itself is mechanically weakened. The material starts to decompose into  $\text{Ag}_2\text{S}$  and sulphurous arsenic compounds, which are volatile at this temperature, and vaporize at the surface regions, leaving residual silver sulphide at the surface of the sample.

The results found in the measurements undertaken give a detailed picture of the externally measurable physical characteristics developed in relation to the silver disorder of the material. However, none of them is able to give a detailed picture of what is actually happening at the atomic scale within the structure, such as where the silver ions disorder to or if they move within the two sets of helical Ag–S spirals or within the chains of silver ions within the structure. It would be interesting to get a more detailed structural picture of the disordered phase, to see whether the pyramids in the structure remain in the same place, for example, or how the disorder of silver affects them, and what happens as the sample decomposes. To clarify some of the structural questions on the behavior and disorder of silver within proustite we plan to use total neutron scattering data to extract the temperature dependence of the radial pair distribution functions of different atom pairs in the structure. By these means a detailed picture of the short-range order may be obtained, parallel to the long-range structure information, to consolidate our work on this system.

<sup>1</sup>K. F. Hulme, O. Jones, P. H. Davies, and M. V. Hobden, *Appl. Phys. Lett.* **10**, 113 (1967).

<sup>2</sup>C. O'Hara, N. M. Shorrocks, R. W. Whatmore, and O. Jones, *J. Phys. D* **15**, 1289 (1982).

<sup>3</sup>S. R. Yang and K. N. R. Taylor, *J. Appl. Phys.* **67**, 3387 (1990).

<sup>4</sup>S. R. Yang and K. N. R. Taylor, *J. Appl. Phys.* **69**, 420 (1991).

<sup>5</sup>P. Toulmin, *Am. Mineral.* **48**, 725 (1963).

<sup>6</sup>P. Engel and W. Novacki, *Acta Crystallogr.* **24**, 77 (1968).

<sup>7</sup>B. Lange, F. Scholz, H. J. Bausch, F. Damaschun, and G. Wappler, *Phys. Chem. Miner.* **19**, 486 (1993).

<sup>8</sup>G. W. Roland, *Econ. Geol.* **65**, 241 (1970).

<sup>9</sup>D. L. Harker, *J. Chem. Phys.* **4**, 381 (1936).

<sup>10</sup>P. Engel and W. Nowacki, *Neues Jahrb. Mineral., Monatsh.* **8**, 181 (1966).

<sup>11</sup>D. G. Semak, I. P. Mikhal'ko, Y. V. Popik, D. M. Bercha, I. I. Nebola, M. I. Golovei, and M. I. Gurzan, *Sov. Phys. Semicond.* **8**, 823 (1975).

<sup>12</sup>S. L. Bravina, A. K. Kadashchuk, N. V. Morozovsky, N. I. Ostapenko, and Y. A. Skryshevsky, *Ferroelectrics* **83**, 119 (1988).

<sup>13</sup>S. R. Yang and K. N. R. Taylor, *Phase Transitions* **36**, 233 (1991).

<sup>14</sup>S. Allen, *Phase Transitions* **6**, 1 (1985).

<sup>15</sup>P. J. S. Ewen, W. Taylor, and G. L. Paul, *J. Phys. C* **16**, 6475 (1983).

<sup>16</sup>R. J. Nelmes, C. J. Howard, T. W. Ryan, W. I. F. David, A. J. Schultz, and P. C. W. Leung, *J. Phys. C* **17**, L861 (1984).

<sup>17</sup>T. W. Ryan, A. Gibaud, and R. J. Nelmes, *J. Phys. C* **18**, 5279 (1985).

<sup>18</sup>J. A. Norcross and D. C. Ailion, *Solid State Commun.* **98**, 119 (1996).

<sup>19</sup>I. M. Shmyt'ko, N. S. Afonikova, N. A. Dorokhova, *Phys. Solid State* **40**, 2013 (1998).

<sup>20</sup>T. Aphi, U. Mikac, J. Seliger, J. Dolinšek, and R. Blinc, *Phys. Rev. Lett.* **80**, 2225 (1998).

<sup>21</sup>R. K. Subramanian, L. Muntean, J. A. Norcross, and D. C. Ailion, *Phys. Rev. B* **61**, 996 (2000).

<sup>22</sup>S. R. Yang, K. N. R. Taylor, and F. Y. Zhang, *J. Phys.: Condens. Matter* **1**, 7669 (1989).

<sup>23</sup>A. D. Belyaev, N. A. Borovoi, Y. P. Gololobov, V. F. Machulin, and E. G. Miselyuk, *Sov. Phys. Solid State* **26**, 1146 (1984).

<sup>24</sup>K. T. Wilke and J. Bohm, *Kristallzüchtung* (Wissenschaft, Berlin, 1988).

<sup>25</sup>A. G. Shtukenberg, Y. O. Punin, O. V. Frank-Kamenetskaya, O. G. Kovalev, and P. B. Sokolov, *Miner. Mag.* **65**, 445 (2001).

<sup>26</sup>A. G. Shtukenberg, Y. O. Punin, and V. N. Soloviev, *Miner. Mag.* **64**, 837 (2000).

<sup>27</sup>A. G. Shtukenberg, D. Y. Popov, and Y. O. Punin, *Miner. Mag.* **66**, 275 (2002).

<sup>28</sup>T. Tanaka, M. Akizuke, and Y. Kudoh, *Miner. Mag.* **66**, 261 (2002).

<sup>29</sup>T. Tanaka, R. Kimura, M. Akizuki, and Y. Kudoh, *Miner. Mag.* **66**, 409 (2002).

<sup>30</sup>D. C. Palmer and E. K. H. Salje, *Phys. Chem. Miner.* **17**, 444 (1990).

<sup>31</sup>K. V. Shcherbin, S. G. Odoulov, B. Sugg, D. Hartmann, M. Neumann, and R. A. Rupp, *Philos. Mag. B* **77**, 3 (1998).

<sup>32</sup>A. C. Larson and R. B. Von Dreele, *GSAS General Structure Analysis System* (LAUR, Los Alamos National Laboratory, Los Alamos, 1994).

<sup>33</sup>M. G. Tucker, D. A. Keen, and M. T. Dove, *Miner. Mag.* **65**, 489 (2001).

<sup>34</sup>A. C. Hannon, *Neutron Diffraction, Instrumentation in Encyclopaedia of Spectroscopy and Spectrometry*, edited by J. C. Lindon, G. E. Tranter, and J. L. Holmes (Academic, New York, 2000).

<sup>35</sup>D. A. Keen and M. T. Dove, *Miner. Mag.* **64**, 447 (2000).

<sup>36</sup>W. Schranz, *Phase Transitions* **64**, 103 (1997).

<sup>37</sup>K. P. Menard, *Dynamic Mechanical Analysis—A practical introduction* (CRC, London, 1999).

<sup>38</sup>J. R. Macdonald, *Impedance Spectroscopy—Emphasizing Solid Materials and Systems* (Wiley, New York, 1987).